J. Plasma Fusion Res. SERIES, Vol. 4 (2001) 253–257

Role of Neutral in ELMy H-Mode Plasmas: 2D Transport Simulation with COCONUT

MIYAMOTO Seiji*, PARAIL Vassili[1], CORRIGAN Gerald[1], HEADING David[1], SPENCE James[1], TARONI Adolfo[2] and HORIIKE Hiroshi

Graduate School of Engineering, Osaka University, Suita 565-0871, Japan

[1]EURATOM/UKAEA Fusion Association, Abingdon, United Kingdom

[2]European Commission, Brussels, Belgium

(Received: 5 December 2000 / Accepted: 24 August 2001)

Abstract

Neutral penetration through SOL is studied for ELMy H-mode plasma with 2D transport code COCONUT, which has been developed at JET Joint undertaking. Interaction between the neutral and the transport barrier is investigated, and it is shown that when increasing gas puffing, sudden increase of ELM frequency can take place and degradation of confinement follows.

Keywords:

ELMy H-mode, modelling of transport barrier, transport simulation, neutral transport, change of ELM frequency

1. Introduction

It is widely known that the ELMy H-mode is commonly observed in various ranges of tokamak devices. In ELMy H-modes, intermittent release of energy and particles appears between H-modes due to several kinds of instabilities [1]. Recently, it was found in JET ELMy H-mode plasmas that a strong gas puffing used to increase density leads to the increase of ELM frequency and following degradation of energy content [2]. Various attempts have been made to explain such behavior [3-5], and it was first pointed out in the reference [3] that this could be explained if we assumed the width of the barrier shrinks with the gas puffing. In the present paper, we show a simulation on neutral penetration through the SOL with a two-dimensional transport code, COCONUT.

At present, theoretical understanding of the H-mode is mainly owing to Itoh [6], Shaing [7] and their coworkers. In Shaing's theory, the orbit loss of trapped particles is considered to play an important role, and transition from L to H-mode is derived from the balance between the orbit loss current and the neoclassical return current. His theory explains some experimental observations quite well [8], but doesn't provide information about the spatial structure of the barrier. A possible estimation of the width of the barrier is that the width is to be proportional to the orbit width of the trapped particles of the highest energy [9], which are probably NBI ions in the case of NBI-heated plasmas.

Based on the theory, one can explain the experimentally observed degradation of confinement and the increase of ELM frequency as follows: the density of NBI ions is determined by the balance between the supply due to diffusion and the loss due to charge exchange. Because the diffusion process is relatively slow compared to the charge exchange process, a strong gas puffing could expel the fast ions completely, and hence the barrier would shrink. Then the shrink of the barrier results in the change of ELM

*Corresponding author's e-mail: miyamoto@nucl.eng.osaka-u.ac.jp

and confinement [3].

To examine this hypothesis, simulations were carried out. The details are described later in the next section, but, to be brief, the result of the simulations did not support the hypothesis. This fact means that another mechanism is needed to explain the shrink of the barrier, but it still has to be explained in the relation to the neutral penetration. In section **3.**, a new model is proposed as to the edge transport barrier. Then an increase of ELM frequency and degradation of confinement are demonstrated. Finally, in section **4.**, the present work will be summarized briefly.

2. Simulation with COCONUT

COCONUT is a two dimensional transport code developed at JET joint undertaking, during past 10 years. The code consists of two parts: one-dimensional transport code, JETTO [10] is used to calculate the transport in the core region, and two-dimensional transport code, EDGE2D [11,12] in SOL, in which magnetic field lines are open. Normally the separatrix of tokamak plasmas is chosen to be the boundary between the calculation regions of the two codes. In the core region of tokamak fusion plasmas, magnetic field lines are closed and magnetic surfaces are formed. Because physical quantities such as temperature or density can be considered as constant on a magnetic surface, the physical quantities in JETTO are solved as a function of magnetic surface with Bohm Gyro-Bohm type transport coefficients [13]. On the other hand, physical quantities in SOL can vary along the magnetic field lines cut off by divertor plates so that the physical quantities in EDGE2D are a function of both magnetic surface and the distance along a magnetic field line. The transport barrier in the code is modeled in a reduction of transport coefficients to its neo-classical value in a narrow region near the plasma edge. An ELM violates this transport barrier. The transport coefficients are suddenly increased in the periphery of the plasma, which is not necessarily the same region as the barrier region. This increase is triggered when the ballooning instability limit is exceeded, and lasts for a short duration. Such a model reproduces experimental trends quite well.

To begin with, three experimental shots were analyzed. In those shots, experimental conditions were all the same except the amount of gas puffing, which was gradually increased shot by shot, 1.4×10^{21} s^{-1} (#39609), 2.1×10^{21} s^{-1} (#39610) and 3.6×10^{21} s^{-1} (#39611). Generally, gas puffing is used as a technique to improve the plasma density, and hence the energy content. It was revealed, however, that an increase of ELM frequency is observed followed by the degradation of confinement when a strong gas puffing is used.

One should be careful before concluding the increase of the frequency is attributable to neutral. The stronger gas puffing doesn't necessarily mean the more neutral penetration, because the gas puffing also raises the SOL plasma density, and the neutral penetration will be blocked off. COCONUT simulation is preferable to handle this problem: SOL density is determined both in consistent with the heat and particle fluxes from the core plasma and in consistent with the neutrals introduced by gas puffing.

In fig. 1, a result from such simulations is shown. The simulations have been done for three different gas puffing rates which correspond to the experiments, and the neutral flux to the core across the separatrix is plotted in the figure. In these runs, the barrier width is prescribed: 3 cm for the shot #39609 and #39610, and 1 cm for #39611. Here, we assumed that the barrier shrinks according to the increase of gas puffing, and ascertained whether the level of the neutral flux that across the separatrix is consistent with the assumption.

To attribute the shrink of the barrier to the charge exchange loss of fast ions, charge exchange rate $\langle \sigma_{CX} v \rangle n^0$, must be much greater than $1/\tau_{sd}$, where σ_{CX} represents charge exchange cross section, n^0 and τ_{sd} the density of the neutral and the slowing down time of the fast ion respectively. The angular brackets mean the average over velocity distribution. From the simulation, the neutral flux increases in the case of strong gas puffing (#39611), but the increase is only about 50%, and neutral density is the order of 10^{15} m^{-3} on the

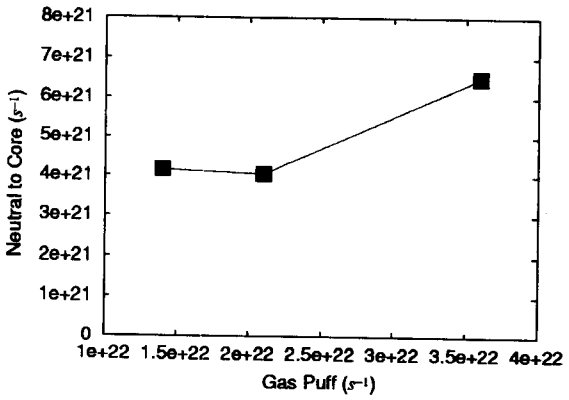

Fig. 1 Neutral flux to core. The three points in the plot correspond to the three experimental cases #39609, #39610 and #39611 from left to right.

separatrix. Estimating that $\sigma_{CX} \sim 10^{-19}$ m^2 and $v_{th} \sim 10^6$ m/s, charge exchange rate is accordingly evaluated as $\langle \sigma_{CX} v \rangle \sim 10^2$ s^{-1}. This evaluation of charge exchange rate is comparable to $1/\tau_{sd}$ of NBI ions, which means the neutral penetration is not sufficient to expel fast ions in the edge. Considering the small change of neutral flux on top of that, it should be concluded that it is hard to attribute the shrink of the barrier to the neutrals.

The reason why the increase of the neutral flux was smaller than that had been expected is the screening effect of SOL. It was observed in the simulation that the plasma density in SOL was increasing in accordance with gas puffing.

3. Reconsideration to the Barrier Width

So far it was assumed that barrier width is constant but changes shot by shot. Here we assume the temporal evolution of the barrier width. It is observed in the simulation that plasma density of SOL drops during ELM, followed by 4–5 times larger neutral penetration to the core. This large neutral flux would expel fast ions from the edge, and hence the width of the barrier will be small just after an ELM. After the ELM, the fast ion will be refilled gradually by the diffusion of NBI ions from core region, which will determine the barrier width, if the following condition is satisfied [9].

$$\frac{n_{\text{fast}}}{n_{\text{th}}} \geq \frac{\rho_{\theta i}}{R}, \qquad (1)$$

where n_{fast} and n_{th} are the density of fast and thermal ion, $\rho_{\theta i}$ the poloidal Larmor radius of thermal ion, and R the major radius of the plasma. Finally, the width of the barrier will reach the poloidal Lamor radius of NBI ions $\rho_{\theta,\text{fast}} = m_i v_{\text{fast}}/eB_\theta$, unless a next ELM is triggered. If the next ELM is triggered so quickly that the condition (1) is not satisfied, then the barrier width remains in the order of $\rho_{\theta i}$, otherwise the barrier width will expand up to the order of $\rho_{\theta,\text{fast}}$.

To see how the above model works, we carried out some more simulation runs with the following transport barrier model:

$$\Delta = \Delta_1 + (\Delta_2 - \Delta_1)\left[1 - \exp\left(-\frac{t - t_{\text{ELM}}}{\tau}\right)\right], \qquad (2)$$

where t_{ELM} is the time at which an ELM terminated. Δ_1 and Δ_2 represent two kinds of scaling of barrier width, $\Delta_1 \sim \rho_{\theta,i}$ and $\Delta_2 \sim \rho_{\theta,\text{fast}}$. We considered τ, which corresponds to a recovering time of NBI ion, changes sensitively to neutral density. Approximately, τ is described as,

$$\frac{1}{\tau} = \frac{1}{\tau_{sd}} - \langle \sigma_{CX} v \rangle n^0. \qquad (3)$$

As mentioned in sec. **2.**, because the first and second terms in r.h.s. of the above equation are the same order, it is consequently possible that small change in neutral would cause large change of τ.

In fig. 2, a result from such a simulation is shown. All the runs were done with 1D code JETTO under fixed boundary conditions. In these runs τ is the parameter of the simulation, where strong gas puffing corresponds to large τ. In the figure, increase of ELM frequency is clearly seen, which could correspond to the experimental observation. The change shows a bifurcational aspect rather than a continuous variation. This bifurcation explains the fast increase of type I ELM frequency with gas puffing reported in the reference [2].

A possible explanation of the bifurcation is schematically shown in figure 3. In the top figure, temporal evolution of the pressure of the pedestal, P and the width of the barrier, Δ is drawn. An ELM ends at t = 0, and then the pedestal pressure starts to recover. At the

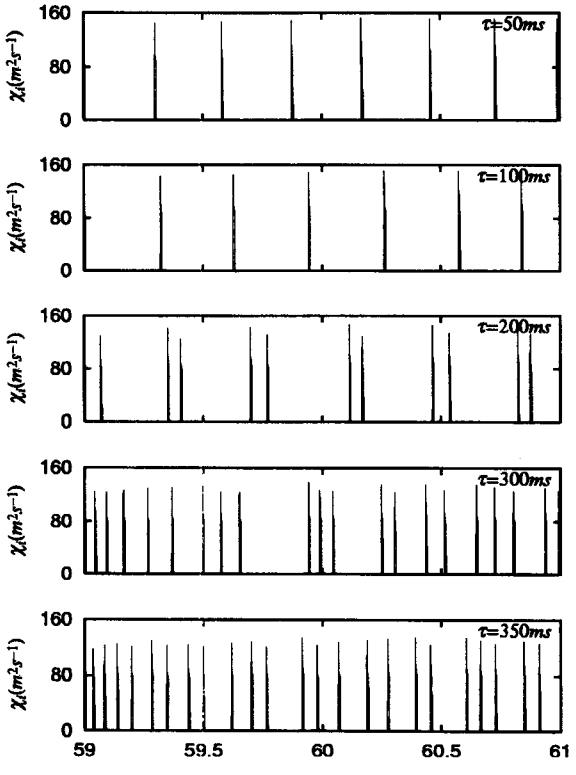

Fig. 2 ELM dependence on recovering time τ. Large τ corresponds to strong gas puffing.

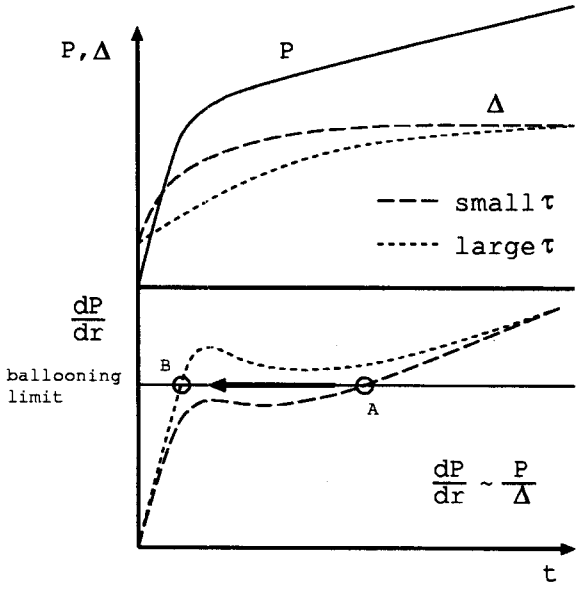

Fig. 3 Schematic drawing of ELM transition mechanism.

initial phase of recovering, the pressure rises quickly, but the speed of the evolution decelerates as the pedestal reaching hydro–dynamical equilibrium. The pressure gradient is estimated as $dP/dr = P/\Delta$. Because the width of the barrier evolves as eq. (2), the pressure gradient goes dip once, and gradually evolves again towards the instability limit (the bottom figure). In the figure, two cases of τ, small and large, are shown. In the case of large τ, because the width of the barrier remains narrow at the initial phase, the pressure gradient hits the instability limit soon. On the other hand, in the case of small τ, because the pressure gradient is reduced due to the fast expansion of barrier, the pressure gradient goes dip without reaching instability limit, and evolves slowly towards the instability limit. The point at which the instability limit is reached is shown by open circles in the case of (A) small τ and (B) large τ. As increased the gas puffing, the point the next ELM is triggered jumps from (A) to (B) at a certain value of τ, hence the ELM repetition period becomes short. This is the mechanism of the bifurcation.

In the reference [2], the authors also reporte a transition of ELM frequency from type I to type III when they used extremely strong gas puffing in the order of 10^{22} s^{-1}. One should note, however, that it is hard to attribute the transition to type III ELM to our model because it requires an unrealistically small Δ_I to reproduce such high frequency ELMs with $f_{ELM} \sim 1$ kHz.

4. Conclusion

Two-dimensional transport code COCONUT was used to analyze the penetration of neutrals through the SOL. In the transport code, transport barrier is modeled in a reduction of transport coefficient to neoclassical value in this region, and ELM is triggered when the pressure gradient exceeds the ideal ballooning limit, which violates the transport barrier. At first, used was the prescribed barrier width in the order of $\rho_{\theta,fast}$ for the weak gas puffing cases and in the order of $\rho_{\theta,i}$ for the strong gas puffing case. Then the dynamics of barrier width was coupled with transport model.

In the case of fixed barrier width, the shrink of the barrier could not be explained based on neutral penetration mechanism, however if the dynamics of barrier width is taken into account, qualitative agreement between experimental results and simulation results are obtained. The crucial point of this model is that the barrier width is determined by the poloidal Larmor radius of thermal ions in the fast time scale, however, it is finally determined by the poloidal Larmor radius of fast ions. If the recovering time of NBI is large enough which corresponds to the strong gas puffing, then the barrier width is dominated by $\rho_{\theta,i}$ since the pressure gradient grows quickly to the ideal ballooning limit, on the other hand, if the recovering time is small, the width could grow in the order of $\rho_{\theta,fast}$. This is the bifurcation mechanism of the frequency in this model. This model explains the experimentally observed fast increase of ELM frequency with gas puffing.

References

[1] H. Zohm, Plasma Phys. Control. Fusion **38**, 105 (1996).

[2] The JET Team (presented by G.F. Matthews), *Proc. of the 17th Fusion Energy Conf, Yokohama 1999*, vol. **1**, 335 (IAEA Vienna 1999).

[3] A. Taroni *et al.*, Contrib. Plasma Phys. **38**, 37 (1998).

[4] H.R. Wilson *et al.*, *Proceedings of the 17th Fusion Energy Conference, Yokohama 1999*, vol. **4**, 1429 (IAEA Vienna 1999)

[5] V. Parail *et al.*, *Proceedings of the 27th EPS Conf. Fus. and Plasma Phys.* (Budapest 2000), *will appear.*

[6] S-I. Itoh and K. Itoh, Phys. Rev. Lett. **60**, 2278 (1988).

[7] K.C. Shaing *et al.*, Plasma Phys. and Contr. Fus. Research, Vol. **2**, 13 (1989), Phys. Rev. Lett. **63**, 2369 (1989), Phys. Fluids B **2**, 1492 (1990).

[8] R.J. Groebner *et al.*, *Proceedings of the 16th European Conference on Controlled Fusion and Plasma Physics*, part **1**, 245 (Venice 1989).

[9] V. Parail, H.Y. Guo and J. Lingertat, Nuclear Fusion, **39**, 369 (1999).

[10] G. Cenacchi and A. Taroni, *The 8th Europhiscs Conf. on Comp. Phys. Eibsee*, 13 (1986).

[11] R. Simonini *et al.*, *Proc. 12th EPS Conf. on Control. Fusion and Plasma Phys.*, Vol. **2**, 484 (1985), Contrib. Plasma Phys. **34**, 368 (1994).

[12] A. Taroni, G. Corrigan, *et al.*, Contrib. Plasma Phys. **32**, 438 (1992).

[13] G. Vlad *et al.*, Nuclear Fusion **38**, 557 (1998).